OPEN

Machine Learning Model for Predicting Visual Acuity Improvement After Intrastromal Corneal Ring Surgery in Patients With Keratoconus

Eva Perez, MD, Nassim Louissi,* Sofiene Kallel, MD,* Quentin Hays, MD,* Nacim Bouheraoua, MD, PhD,* Malika Hamrani,* Anatole Chessel, PhD,† and Vincent Borderie, MD, PhD**

Background: Keratoconus is a progressive, degenerative corneal disease that can lead to significant visual impairment. The intrastromal ring segment implantation procedure is effective in reshaping the cornea and improving vision. However, vision does not improve postoperatively in all operated eyes, and the results vary widely among patients, making it challenging to predict postoperative visual gain.

Purpose: This study investigated the potential of machine learning in predicting postoperative visual acuity in keratoconus patients undergoing intrastromal ring segment implantation with the aim of enhancing surgical decision-making.

Methods: This retrospective study analyzed 120 eyes of 102 patients with keratoconus who underwent ring segment implantation (1 symmetric or asymmetric segment, 150–300 μm thick, 150 degrees, or 160 degrees-arc). Preoperative and postoperative refraction, corneal topography, and tomographic data were collected. Various models were trained to predict postoperative visual acuity improvements.

Results: The models demonstrated excellent performance, with XGBoost achieving perfect results in predicting whether vision will improve after surgery (R^2 = 1.0, Youden Index = 1.0; all test observations being correctly classified). The CatBoost model achieved an R^2 of 0.59 [0.7-line mean absolute error (MAE)] for predicting postoperative visual acuity, an R^2 of 0.76 (MAE, 1.08 D) for predicting keratometry, and an R^2 of 0.54 (MAE, 0.29) for predicting corneal asphericity. Key features for accurate predictions included preoperative keratometry values (K1, K2, Kmax), corneal asphericity, and visual acuity, whereas segment characteristics featured low importance.

Conclusions: This study shows the strong potential of machine learning for selecting candidates for surgery and predicting postoperative visual improvements after ring segment implantation in keratoconus eyes.

Key Words: keratoconus, intrastromal corneal ring segments, corneal topography, machine learning, artificial intelligence

(*Cornea* 2025;00:1–11)

Keratoconus is a progressive, noninflammatory corneal disease characterized by thinning and ectasia that may progress to irregular astigmatism, myopia, and vision loss if left untreated.[1,2] It typically manifests during adolescence and is influenced by genetic predisposition, mechanical eye rubbing, and ocular allergies.[3,4] While early stages can be managed with corrective lenses or rigid contact lenses, advanced cases often require more invasive surgical interventions, including corneal collagen crosslinking,[5] intrastromal ring segment implantation, and, in more severe cases, corneal transplantation.

Intrastromal ring segments represent a safe, reversible, and stable surgical procedure that can correct corneal ectasia by flattening the cornea and improving its shape.[6,7] Intracorneal ring segment can reduce the need for more invasive treatments, such as corneal grafts, in patients with keratoconus.[8] These crescent-shaped polymethylmethacrylate implants are placed in the corneal stroma and have been shown to reshape the cornea and improve visual function effectively.[9] Recently, donor allogeneic corneal tissue has been

Received for publication March 14, 2025; revision received May 18, 2025; accepted May 24, 2025.

From the *GRC 32, Transplantation et Thérapies Innovantes de La Cornée, TTIC, Hôpital National des 15-20, Sorbonne Université, Paris, France; and †Laboratory for Optics and Biosciences (LOB), École Polytechnique, CNRS, Inserm, Institut Polytechnique de Paris, Palaiseau, France.

Supported by Agence Nationale de la Recherche (grant #ANR-21-CE19-0010-02, CorMecha project). The sponsor or funding organization had no role in the design or conduct of this research.

The authors have no financial or proprietary interest in any material or method mentioned in this paper.

Design of the study (E. Perez, N. Louissi, V. Borderie); conduct of the study (E. Perez, N. Louissi, S. Kallel, Q. Hays, N. Bouheraoua, A. Chessel, V. Borderie); collection, management, management, analysis, and interpretation of data (E. Perez, N. Louissi, M. Hamrani, N. Bouheraoua, A. Chessel, V. Borderie); preparation, review, and approval of manuscript (E. Perez, N. Louissi, S. Kallel, Q. Hays, N. Bouheraoua, A. Chessel, V. Borderie).

E. Perez and N. Louissi have contributed equally.

Correspondence: Vincent Borderie, MD, PhD, Hôpital National des 15-20, 28 Rue de Charenton, Paris 75571, France (e-mail: vincent.borderie@upmc.fr).

proposed to produce intrastromal ring segments.[10] A major challenge in using intrastromal ring segments is the unpredictability of patient outcomes. Individual variations in corneal biomechanics, healing responses, and disease progression make it difficult for surgeons to consistently forecast the refractive, topographic, and biomechanical results after surgery.[11]

Recent advancements in artificial intelligence (AI),[12–15] particularly in machine learning (ML), have opened new possibilities in the field of ophthalmology.[16] AI-driven approaches, such as artificial neural networks, have already been applied in diagnostics and predictive modeling across various medical fields. ANNs mimic the learning processes of biological neural systems, allowing them to analyze large datasets, recognize patterns, and develop predictive models. By training on real-life cases stored in databases, these networks can generalize knowledge and make predictions for new cases, which makes them highly valuable in medical decision-making.[17,18]

In ophthalmology, ML algorithms have shown great promise in detecting and classifying keratoconus using corneal imaging and diagnostics data.[19–26] Beyond keratoconus, AI has been applied to a broad spectrum of anterior segment diseases, including infectious keratitis, corneal transplantation, cataract surgery, angle-closure glaucoma, and iris tumors, assisting in diagnosis, staging, and treatment planning.[27] For example, in infectious keratitis, convolutional neural networks (CNNs) have been trained on slitlamp and OCT images to automatically detect and classify corneal infections, improving diagnostic accuracy. In refractive and cataract surgery, AI models such as gradient boosting machines and neural networks have been applied to optimize intraocular lens power calculations by learning complex relationships between biometric parameters and postoperative refractive outcomes, surpassing the accuracy of traditional formulas.[28,29]

However, using ML to predict surgical outcomes, such as visual acuity improvements following ring segment implantation, remains relatively underexplored. Predicting postoperative outcomes is particularly important for optimizing treatment plans and improving patient care, as it allows surgeons to better tailor the procedure to each patient's needs.

This study addresses this gap by developing a machine learning model to predict visual acuity gains in patients with keratoconus after ring segment implantation. By using preoperative and postoperative refractive and corneal topography data, the model aims to provide personalized predictions for the best possible outcomes, considering the unique characteristics of each patient's corneal structure. This approach could enable selecting patients for surgery, more precise planning of procedures, and optimizing the segment's number, placement, and configuration to achieve the most favorable refractive and topographical results. It could revolutionize surgical decision-making in keratoconus treatment, significantly improving patient outcomes and reducing variability in postoperative results.

MATERIALS AND METHODS

Study Design and Population

This retrospective, single-center study included 120 eyes of 102 patients with keratoconus who underwent ring segment implantation between January 2021 and January 2024 at the French National Vision Hospital (Hôpital National de la Vision des 15–20), Paris, France.

Inclusion criteria were the following: patients with a diagnosis of keratoconus who had undergone ring segment implantation with either symmetric (FERRARA RING, AJL Ophthalmic, Spain) or asymmetric (AJL PRO+, AJL Ophthalmic, Spain; INTRASEG, EmmetropR, France) segments, with an arc of 150 degrees or 160 degrees and a thickness between 150 and 300 μm, complete preoperative and postoperative corneal topography/tomography data available. Asymmetric segments labeled as 150 μm or 200 μm feature a 100-μm-thick thin end, and segments labeled as 250 μm or 300 μm feature a 150-μm-thick thin end. The ring was chosen based on the manufacturer's nomograms (Intraseg, Ferrara, and AJL) and mainly the surgeon's clinical judgment. Exclusion criteria included patients with other corneal disorders (ie, pellucid marginal degeneration or post-LASIK ectasia), those with incomplete postoperative data, and those who underwent other simultaneous corneal procedures such as cross-linking.

Ethics Statement

The described research adhered to the tenets of the Declaration of Helsinki. All patients were included in the CCK-CONE cohort study following informed consent. Ethics committee approval was obtained from the INDS (Institut National des Données de Santé, #255645) following approval by the CEREES (February 13, 2020). The data protection process agreed with the reference methodology MR-004, and the CNIL approved the conformity declaration (March 23, 2020). The cohort protocol is available on the Health Data Hub (https://www.health-data-hub.fr/projets/observatoire-de-la-prise-en-charge-des-patients-presentant-un-keratocone-du-centre-de).

Surgical Technique

All procedures were performed under topical anesthesia. The center of the pupil was marked, and a disposable suction ring was positioned accordingly. A femtosecond laser (Wavelight FS 200, Alcon Laboratories, Inc) created a channel at a depth of 75% of the corneal thickness. The incision was aligned with the axis of the steepest keratometry. The inner and outer diameters of the channel were, respectively, on average, 4.59 mm (±0.26) and 5.81 mm (±0.23) for 5 mm ring segments, and 5.71 mm (±0.24) and 7.47 mm (±0.53) for 6 mm ring segments, depending on the preferences of each surgeon.

The laser settings were customized for the specific ring segment type. The energy used to create the channel and incision was set at 1.20 mJ. The segments were implanted using forceps under sterile conditions. The final placement of the segments was adjusted using a Sinskey hook.

Postoperative care included a combination of antibiotic (tobramycin 3 mg/mL) and steroid (dexamethasone 1 mg/mL) eye drops (Tobradex; Alcon Laboratories Inc., Fort Worth, TX), applied 3 times daily for 2 weeks. In addition, patients

were instructed to use tear substitutes (Vismed, Horus Pharma, Nice, France) for 1 month following the procedure.

Data Collection

Preoperative and postoperative data were collected from 2 primary sources

Refractive Data

This included uncorrected visual acuity, distance-corrected visual acuity (DCVA), spherical equivalent, cylinder, and axis measurements obtained through subjective refraction. Visual acuity was measured using a decimal chart and converted to logarithm of the minimum angle of resolution (LogMAR) units.

Corneal Topography/Tomography Data

Corneal topography data were collected using the MS-39 corneal topographer/tomographer (CSO, Firenze, Italy), which combines a Placido disc-based topographer and a spectral domain optical coherence tomographer, and provides detailed measurements of corneal curvature [mean keratometry in the 3 mm central zone (Kmean), keratometry in the flattest meridian for the 3 mm central zone (K1), keratometry in the steepest meridian for the 3 mm central zone (K2), and maximum keratometry (Kmax)].

In addition, we measured the minimal corneal thickness (ThkMin) and corneal aberrations. The MS-39 software EyeTop2005 (CSO) automatically converts the corneal elevation profile into corneal wavefront data using Zernike polynomials, expanded to the seventh order. In this study, the root mean square values for a 5 mm pupil were calculated for the following types of aberrations: total, higher-order aberrations, particularly coma, and asphericity (Q-value).

The MS-39 generates CSV files containing quantitative data for various corneal parameters and topography maps visually depicting corneal curvature and elevation. The MS-39 device generates 16 different topography maps, covering various aspects of corneal geometry and refractive properties, that is, Anterior Tangential Curvature (mm), Anterior Sagittal Curvature (mm), Anterior Gaussian Curvature (mm), Anterior Frontal Refractive Power (D), Posterior Frontal Refractive Power (D), Equivalent Refractive Power (D), Corneal Thickness (μm), Stromal Thickness (μm), Epithelial Thickness (μm), Anterior Chamber Depth (mm), Posterior Tangential Curvature (mm), Posterior Sagittal Curvature (mm), Posterior Gaussian Curvature (mm), Anterior Elevation (mm), Posterior Elevation (mm), Stromal Elevation (mm). We selected the first 11 16 maps for our CNN models, focusing on those most relevant. We excluded maps such as posterior sagittal and posterior Gaussian curvature because the models did not achieve satisfactory reconstruction performance for these maps.

Data Preprocessing and Feature Engineering

Given the complex, high-dimensional nature of the data, we applied several preprocessing and feature engineering steps to prepare the dataset for ML analysis.

Data Integration

We assembled 3 primary data sources for each patient: refractive data, MS-39 CSV files containing corneal parameters and MS-39 topography maps.

Transformation of MS-39 CSV Data

The raw CSV files from the MS-39 device contain multiple corneal parameters, including corneal thickness, keratometry, and curvature. To extract meaningful information, we computed several statistical measures for each parameter: minimum, maximum, and mean values, variance, 25th and 75th percentiles (quant25 and quant75), skewness, and kurtosis. This transformation resulted in 196 distinct features per patient, capturing the variability and distribution of corneal characteristics.

Topography Map Reconstruction

In addition to numerical data, we reconstructed 11 of the 16 available MS-39 topography maps for analysis with CNNs. These maps were normalized and resized to a standard resolution to ensure compatibility with CNN architectures.

Feature Selection for Prediction

Several outcome measurements were used to train AI algorithms, which were either binary or quantitative.

Procedure success (binary feature) was determined according to the postoperative change in visual acuity. We calculated the difference in LogMAR visual acuity before and after the procedure as a critical metric of surgical success. The procedure was successful if the gain in corrected visual acuity was strictly greater than 1 line.

The following key postoperative outcome quantitative variables were also analyzed: LogMAR DCVA, refractive cylinder, keratometry (K1, K2, Kmax), corneal asphericity (Q-value), corneal coma.

Data Normalization

All continuous variables were normalized using z-score normalization to standardize the input data. One-hot encoding was applied to any categorical features.

Handling Missing Data

For missing data points, we used median imputation techniques to preserve the sample size.

ML Models and Analysis

We used a combination of ML techniques for classification and regression tasks, using cross-validation to ensure robustness and generalizability. We also stratified target variables for our Classification task. We split the dataset using 70% training, 15% validation, and 15% testing and applied 3-fold cross-validation to evaluate model performance.

Classification Model

We developed a binary classification model to predict whether a patient would gain more than 1 visual acuity line

postoperatively. This task used Gradient-Boosting Classifiers from the XGBoost library, which are highly effective for structured tabular data. The input features included preoperative MS-39 data, refractive measurements, and derived statistical metrics from the CSV files. We performed hyperparameter tuning using grid search with 3-fold cross-validation. Performance was evaluated using the R^2 score and Youden index. $R^2 = 1$ and Youden Index = 1 indicate optimal results.

Regression Models

We used 1 primary regression model (CatBoost) to predict specific postoperative outcomes (ie, LogMAR, keratometry, asphericity). This gradient-boosting algorithm was used to predict postoperative keratometry, LogMAR visual acuity, and corneal asphericity. It effectively handles categorical features and can model nonlinear relations between variables.

CNNs

To leverage the spatial information in the reconstructed MS-39 topography maps, we developed CNN models to analyze these maps and predict postoperative outcomes directly. First, each variable from the MS-39 tool was transformed from polar to Cartesian coordinates, resulting in a 256 × 256 Cartesian matrix for each variable. Gaps in the data were interpolated using cubic interpolation. The images were then rebuilt using the Matplotlib library in Python. Afterward, we structured and integrated each patient image, labeling them with their actual values so the model could compare them to its predictions. The CNN model was based on a modified VGG16 architecture implemented with the PyTorch framework. The CNN model consists of multiple convolutional layers, max-pooling, and fully connected layers. Dropout was used to prevent overfitting. We iterated our model while tweaking different combinations of optimizers (Adam, AdamW, Adagrad) and learning rates. AdamW, paired with a 1e-2 learning rate, yielded the best results.

Model Validation

We split the dataset using 70% training, 15% validation, and 15% testing and applied 3-fold cross-validation to evaluate model performance.

Feature Importance

Feature importance was assessed using built-in methods of XGBoost and CatBoost, allowing us to identify the most important predictors of visual acuity gain. Principal Component Analysis was applied to reduce dimensionality and improve model performance.

Statistical Analysis

In addition to the ML analysis, we conducted conventional statistical tests to understand the relationships between variables better. We calculated the mean, median, and SD for all continuous variables and the frequencies for categorical variables. The Mann-Whitney *U* test was used to compare quantitative variables between patient groups (eg, those who gained more than 1 line of visual acuity vs. those who did not). Spearman rank correlation coefficients assessed the relationships between corneal parameters and visual outcomes.

RESULTS

Study Population

The study included 120 eyes from 102 consecutive patients diagnosed with keratoconus, including 59 female (59%) and 43 male patients (41%). The average age at the time of presentation was 33 years. Considering the Amsler-Krumeich classification, there were 48 grade 1 keratoconus (40%), 54 grade 2 (45%), 15 grade 3 (12.5%), and 3 grade 4 (2.5%). Out of 120 procedures, 111 eyes (92.5%) underwent implantation of asymmetric ring segments, including fourteen 300-μm thick segments (12.6%) and eighty-seven 250-μm thick segments (78.4%), nine 200-μm thick segments (8.1%), and one 150-μm thick segment (0.9%), with the following arc length: 160 degrees (71, 64.0%) and 150 degrees (40, 36.0%). Nine eyes (7.5%) received symmetric segments, including seven 250-μm thick segments (77.8%), one 200-μm thick segment (11.1%), and one 150-μm thick segment (11.1%), with the following arc length: 160 degrees (8, 88.9%) and 150 degrees (1, 11.1%). No intraoperative or postoperative complications were reported during the follow-up.

Descriptive Data Summary

Table 1 shows the eye characteristics before and after ring segment implantation. Postoperatively, a significant improvement was observed in DCVA, with an average gain of 2.0 ± 1.4 lines. Out of 120 eyes, 88 (73.4%) had an improvement of at least 2 lines (range +2 to +7 lines), 31 (25.8%) had no improvement (range −1 to +1 line), and 1 eye (0.8%) lost 2 lines of DCVA. The refractive cylinder decreased by 1.84 ± 2.06 D on average. The mean keratometry decreased by 2.86 ± 4.26 D, and the minimum corneal thickness increased by 17.3 ± 13.5 μm (approximately 4%) on average. The asphericity index (Q-value) and coma aberration decreased by, respectively, 0.50 + 0.45 and 0.68 + 0.74 μm on average.

Classification Model Performance

The Gradient-Boosting Classifiers from the XGBoost library showed excellent performance in predicting whether patients would gain strictly more than 1 line of visual acuity postoperatively (R^2, 1.0; Youden Index, 1.0). These results indicate perfect discrimination between the 2 patient groups, though, due to the small sample size, caution should be exercised regarding potential overfitting. Table 2 shows the 10 most important parameters in differentiating patients with improved visual acuity and those without vision improvement.

Regression Model Performance

The CatBoost regression models demonstrated strong predictive capabilities for postoperative visual outcomes. LogMAR DCVA: the mean absolute error (MAE) was 0.07 corresponding to approximately 0.7 lines of visual acuity,

TABLE 1. Preoperative and Postoperative Characteristics of 120 Keratoconus Eyes With Intracorneal Ring Segment Implantation

	Pre-operative Assessment	Postoperative Assessment	Difference	*P* (Wilcoxon Signed-Rank Test)
DCVA (LogMAR)	0.30 ± 0.19 (20/32+1.9 line)	0.10 ± 0.12 (20/25+1.2 line)	0.20 ± 0.14 (+2.0+1.4 lines)	<0.000001
Sphere (D)	−2.20 ± 2.78	−0.61 ± 2.59	1.58 ± 2.60	<0.000001
Cylinder (D)	−3.65 ± 1.87	−1.80 ± 1.10	1.84 ± 2.06	<0.000001
SE (D)	−4.03 ± 3.07	−1.53 ± 2.67	2.51 ± 2.80	<0.000001
Kmean (D)	48.03 ± 3.30	45.54 ± 3.08	−2.86 ± 4.26	<0.000001
Kmax (D)	59.97 ± 37.59	59.47 ± 7.30	−0.50 ± 37.80	0.001
ThkMin (μm)	436 ± 35.72	454 ± 35.99	17.3 ± 13.5	<0.000001
Q value	−0.96 ± 0.49	−0.46 ± 0.63	0.50 ± 0.45	<0.000001
Coma (μm)	1.75 ± 0.71	1.06 ± 0.60	−0.68 ± 0.74	<0.000001

The mean values and their SD are shown.

Coma, total coma centered on the pupil within the central 5 mm; Kmean, mean keratometry of the central 3 mm; Kmax, maximum keratometry; SE, spherical equivalence; ThkMin, minimum corneal thickness; Q value, asphericity index of the anterior surface of the central 8 mm.

with an R^2 of 0.59, indicating that 59% of the variance in postoperative visual acuity was explained by preoperative data (Fig. 1). This result is nuanced with a 0.099 (0.99 line) root mean square error (RMSE), which penalizes high errors. Mean Keratometry: the model achieved an R^2 of 0.76, indicating that the pre-operative data could explain 76% of the variance in postoperative keratometry. MAE (1.08 D) and RMSE (1.52 D) confirmed the model's robust predictive power for this metric (Fig. 2). Corneal Asphericity (Q-value): R^2 was 0.54 with a 0.29-MAE and a 0.38-RMSE, suggesting moderate predictive capability for this output(Fig. 3).

CNN Performance

The CNN models demonstrated fewer promising results than traditional ML models. For LogMAR DCVA, the CNN model achieved a test R^2 of 0.10, with a test RMSE of 0.11 (1.1 line) and a test MAE of 0.09 (0.9 line), indicating moderate predictive accuracy. Regarding Mean Keratometry, predictions featured a lower R^2 of 0.05, with a test RMSE of 2.10 D and a test MAE of 1.84 D, reflecting less precise performance. Concerning Q-Value, the model's performance was the weakest, with an R^2 of 0.02, a test RMSE of 0.61, and a test MAE of 0.49, highlighting significant challenges in prediction accuracy for this metric.

CNN architecture was particularly effective at capturing spatial patterns in the corneal maps that were not evident in the scalar features used in the traditional ML models.

Table 3 compares the performance of CatBoost and CNN models across different predictive tasks, including postoperative visual acuity (LogMAR DCVA), mean keratometry, and corneal asphericity (Q-value). The CatBoost model demonstrated superior accuracy for all targets, particularly for predicting keratometry ($R^2 = 0.76$) and visual acuity ($R^2 = 0.59$, MAE $\approx$ 0.7 lines). In contrast, the CNN model showed lower predictive performance.

Feature Importance

The top 10 most critical preoperative features contributing to the model's predictions for postoperative LogMAR were ranked by relative importance (Fig. 1). The LogMAR DCVA demonstrated the highest importance, followed by the minimum anterior elevation and the asymmetrical ring type.

TABLE 2. Ten Most Important Predictive Factors of Postoperative Visual Improvement

Feature	Eyes With at Least 2 Lines of Visual Improvement (n = 88)	Eyes With 1 Line or Less of Visual Improvement (n = 32)	*P**
LogMAR DCVA	0.37 ± 0.19 (20/46 + 1.9 line)	0.14 ± 0.09 (20/28 + 0.9 line)	<0.0001
Minimum anterior elevation (μm)	0.00 ± 0.00	0.00 ± 0.00	0.44
Asymmetric ferrara ring	83/88 (94%)	28/32 (87%)	0.24
Minimum anterior chamber depth (mm)	1.01 ± 0.27	1.00 ± 0.35	0.63
Steep keratometry (D)	50.98 ± 3.65	49.29 ± 3.46	0.02
Minimum stromal elevation (μm)	0.05 ± 0.01	0.05 ± 0.01	0.31
75th percentile of the posterior tangential radius of curvature (mm)	8.26 ± 1.29	8.57 ± 1.17	0.07
75th percentile of the stromal elevation (μm)	0.99 ± 0.11	1.01 ± 0.11	0.22
Corneal thickness skewness (μm)	0.44 ± 0.31	0.38 ± 0.31	0.21
Minimum posterior Gaussian refractive power (D)	0.38 ± 0.31	4.28 ± 0.55	0.16

The features are ranked by importance in the predictive model. For quantitative features, the mean values and their SD are shown. For categorical features, numbers and percentages are shown.

*Mann-Whitney test for quantitative features, Fisher exact test for qualitative features.

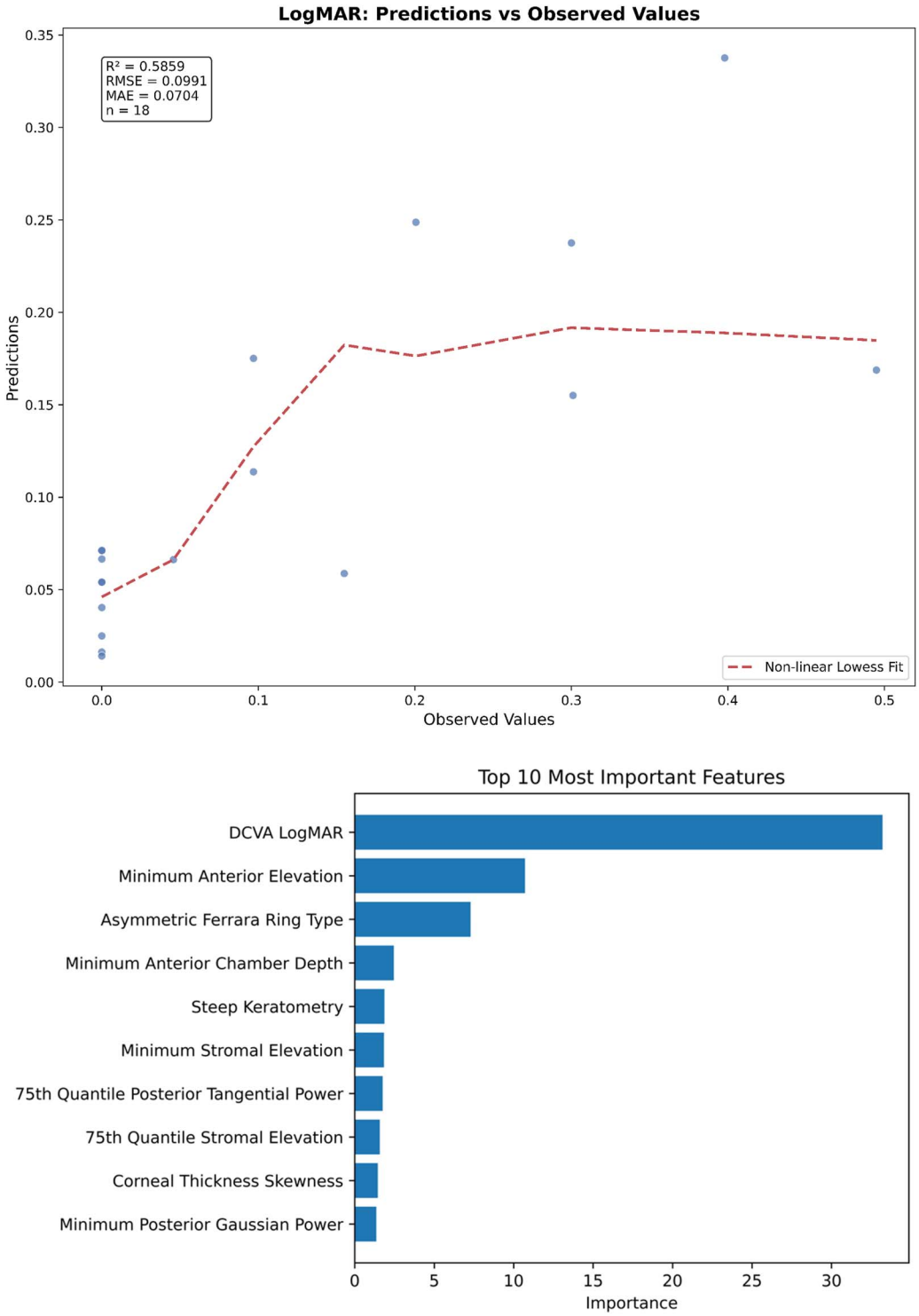

FIGURE 1. LogMAR distance-corrected visual acuity in the test set. A, Predicted versus observed values (CatBoost Model). Blue dots represent CatBoost predictions compared with observed postoperative DCVA values. The red dashed line shows a LOWESS (locally weighted scatterplot smoothing) fit to detect potential nonlinear deviations from the ideal prediction line (y = x). B, Top 10 most important preoperative features in the model. Based on their importance score, this bar chart ranks the top 10 most important features contributing to the model's performance.

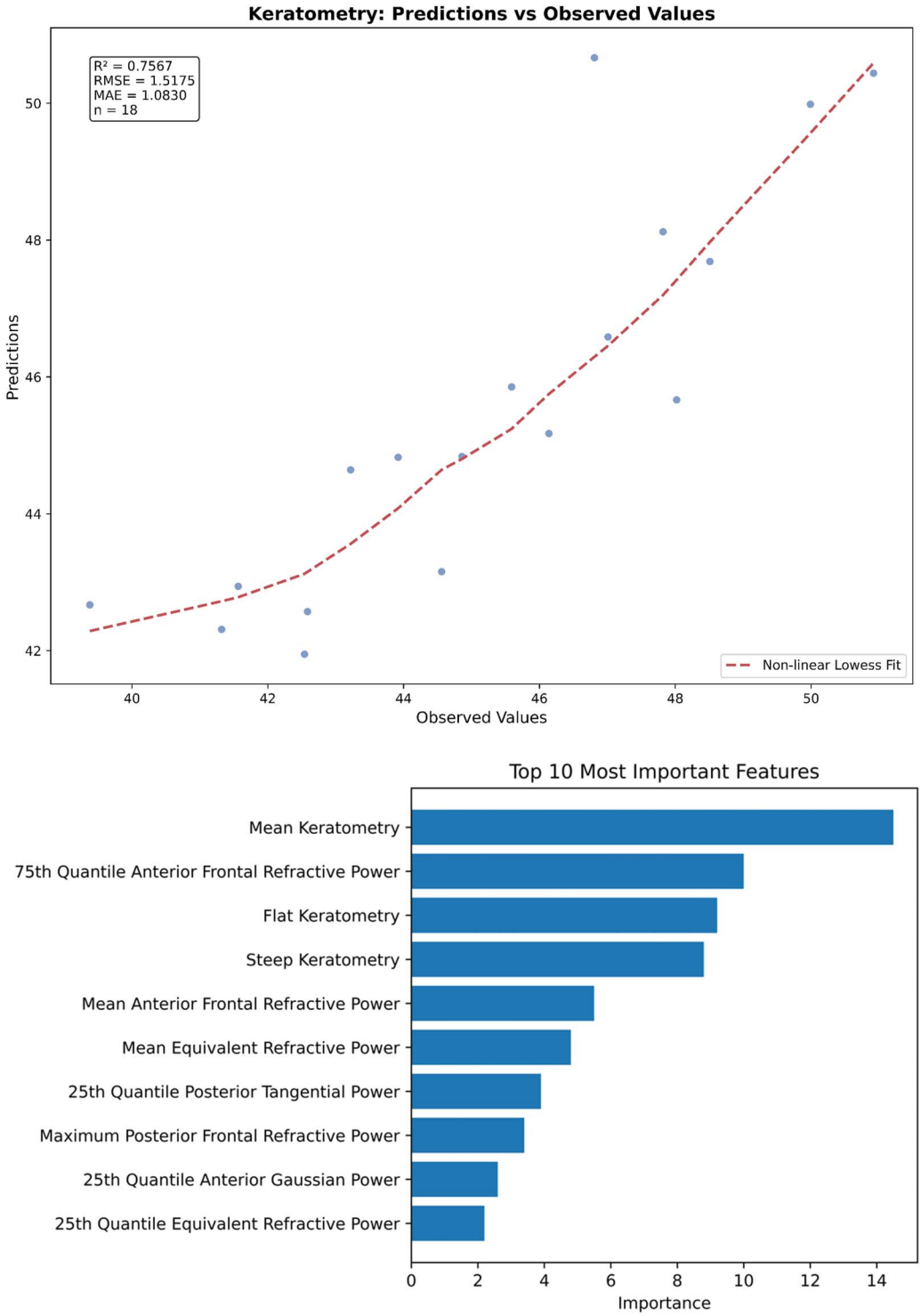

FIGURE 2. Mean keratometry in the test set. A, Predicted versus observed values (CatBoost model). Blue dots represent CatBoost predictions compared with observed postoperative DCVA values. The red dashed line shows a LOWESS (locally weighted scatterplot smoothing) fit to detect potential nonlinear deviations from the ideal prediction line (y = x). B, Top 10 most important preoperative features in the model.

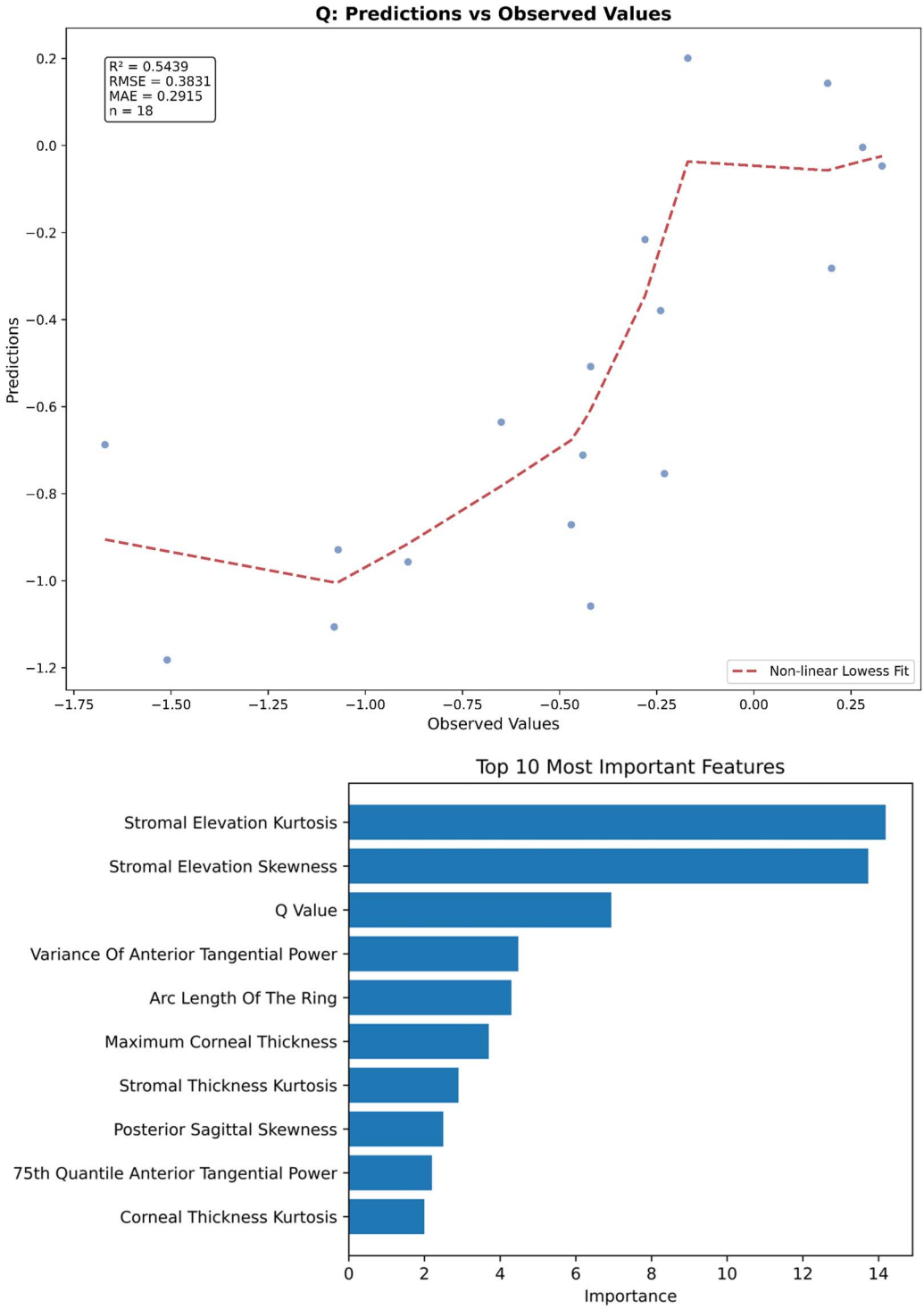

FIGURE 3. Asphericity (Q) in the test set. A, Predicted versus observed values (CatBoost model). Blue dots represent CatBoost predictions compared with observed postoperative DCVA values. The red dashed line shows a LOWESS (locally weighted scatterplot smoothing) fit to detect potential nonlinear deviations from the ideal prediction line (y = x). B, Top 10 most important preoperative features in the model.

TABLE 3. Results of Machine Learning Algorithms and Convolutional Neural Networks for Predicting Postoperative Visual Acuity, Keratometry, and Corneal Asphericity

Feature	Model	R^2	Mean Absolute Error	Root Mean Square Error
LogMAR DCVA	CatBoost	0.59	0.07 (0.7 line)	0.099 (0.99 line)
LogMAR DCVA	CNN	0.10	0.09 (0.9 line)	0.11 (1.1 line)
Mean keratometry (D)	CatBoost	0.76	1.08	2.10
Mean keratometry (D)	CNN	0.05	1.84	2.10
Asphericity (Q-value)	CatBoost	0.54	0.29	0.38
Asphericity (Q-value)	CNN	0.02	0.49	0.61

Figure 2 shows the top 10 most important features for predicting postoperative mean keratometry. Preoperative mean keratometry was the most important feature, substantially impacting the model's predictive accuracy.

Figure 3 shows the top 10 most important features for postoperative Q-value predictions. The stromal elevation kurtosis was the most important feature, closely followed by the stromal elevation skewness. In addition, the reconstructed topography maps contributed to improved predictions when incorporated into the CNN models.

DISCUSSION

In the present study, ML models could efficiently predict which patients would benefit from intrastromal ring segment implantation. Predicting whether a keratoconus eye will significantly improve vision after ring segment implantation is essential for selecting candidates for surgery and avoiding unsuccessful procedures. The Gradient Boosting Classifier model showed perfect performance in predicting whether patients would gain strictly more than 1 line of visual acuity postoperatively (R^2, 1.0; Youden Index, 1.0, meaning all test observations were correctly classified). R^2 represents the proportion of variability in postoperative visual acuity explained by the model, indicating its goodness of fit, while the Youden Index combines sensitivity and specificity to assess the model's classification performance. The 5 parameters featuring the highest importance in the model were the preoperative DCVA, the minimum value of the anterior elevation, whether an asymmetric ring had been used, the minimum value of the anterior chamber depth, and the steep keratometry of the central 3 mm. Patients with preoperative poorer visual acuity and steeper corneas and who received asymmetric rings were more likely to improve vision after surgery. The Amsler-Krumeich classification and keratoconus pattern types (central nipple, crescent, duck, etc.) provided by the MS-39 were included in the dataset, but they showed limited predictive importance in our models.

This study highlights the potential of ML models, particularly CatBoost, in predicting postoperative visual acuity gains in patients with keratoconus undergoing intracorneal ring segment implantation. The models demonstrated significant predictive accuracy, with R^2 values reaching 0.76 for keratometry and mean absolute errors of less than 1 line on the LogMAR chart for visual acuity. These results agree with previous studies, such as those conducted by Vega-Estrada et al[30] and Valdés-Mas et al,[31] which have shown that artificial neural networks and ML algorithms can improve the predictability of outcomes like corneal curvature (K1) and astigmatism after ring segment implantation. The present study provides further important information by predicting the improvement in visual acuity.

The improvement of the ML models in this study, particularly in predicting visual acuity and keratometric changes, underscores the value of advanced analytics in clinical ophthalmology. For example, Vega-Estrada et al demonstrated that ANN-guided ring segment implantation led to better spectacle-corrected distance visual acuity and a significant reduction in coma-like aberrations compared to traditional nomograms. Similarly, Valdés-Mas et al highlighted the importance of key parameters like keratometry and the depth position of the ring in accurately predicting postsurgical outcomes in patients with keratoconus. Lyra et al[32] evaluated the predictability of asphericity and average keratometry in keratoconus patients after ring segment implantation using AI. The study demonstrated that computational models could enhance accuracy and support better surgical decision-making, ultimately improving clinical outcomes for patients with keratoconus. In the present study, we could predict which patients will likely achieve significant visual improvement from the surgery, allowing for a more accurate selection of candidates who would benefit from the procedure.

The feature importance analysis from our study underscores the significant role of specific corneal measurements—keratometry values (K1, K2, Kmax), corneal asphericity, and pre-operative LogMAR visual acuity—in predicting postoperative visual outcomes. Interestingly, the analysis indicates a minimal contribution from the parameters related to the ring itself, such as those describing its dimensions or placement. This suggests that while the rings are integral to the surgical procedure, their variations may not significantly influence the outcome as much as the intrinsic properties of the cornea itself and the preoperative vision level.[11,33]

The outcomes from the descriptive data are consistent with findings reported in other studies on this topic,[34,35] reinforcing their validity.

However, despite the promising results, this study shares common limitations with other AI-based research. First, the small sample size results in low power, and the single-center nature of the study limits the generalizability of the findings. While statistically significant, the results would benefit from validation in more extensive, multicenter trials. This issue of limited data size is frequently encountered in AI research. A larger dataset would likely reduce model variance and enhance the robustness of predictions, especially when evaluating complex conditions like keratoconus. Our results only apply to eyes treated with a single ring ranging from 150 to 160 degrees in angular length and 150 to 300 μm in thickness. Consequently, our models cannot predict postoperative results if rings featuring other sizes and lengths

were to be used. If our models were to be used in different centers, a local training set would be needed to fit and validate the models.

Another important limitation is the potential overfitting observed in some models. The high performance of the XGBoost classifier (R^2 = 1.0, Youden Index = 1.0) suggests that the model may have learned patterns too specific to the training dataset, reducing its generalization ability. For this reason, we chose to present the CatBoost model results, which, although less optimal, provide a more realistic and reliable estimate of predictive performance given the limited sample size. External validation on larger, more diverse patient populations is necessary to confirm its robustness and ensure clinical applicability.

Moreover, the black-box nature of specific ML models, particularly CNNs, presents another challenge. Although CNNs have shown superior performance in image-based predictions, their lack of interpretability limits immediate clinical adoption. This limitation was also noted in Ferrara et al's study, where linear regression models were favored for their transparency despite potentially lower predictive power compared to more complex algorithms like CNNs.[36,37] In the present study, ML models were more efficient than CNN in predicting postoperative visual acuity, mean keratometry, and corneal asphericity. The small data set (CNNs typically require large amounts of data for correct training) and data noise (ie, corneal topographic maps may contain artifacts or inaccurate measurements that may degrade CNN performance) may explain this unexpected result in Table 3.

In addition, the need for calibration from ML models poses a critical limitation in ophthalmology. Many ML models lack proper calibration. Conformal prediction techniques address this limitation by providing valid prediction intervals, thereby enhancing the trustworthiness of model outputs.

Despite these challenges, the study marks a significant step forward in using ML for keratoconus treatment planning.

In conclusion, ML models hold great promise for improving personalized treatment planning in patients with keratoconus undergoing ring segment implantation. As data sets grow and model transparency improves, these tools could become integral to clinical practice, enabling ophthalmologists to predict surgical outcomes better, optimize patient care, and reduce variability in postoperative results. Future research should focus on expanding data sets, validating findings across multiple centers, and enhancing the interpretability of ML models to facilitate broader clinical acceptance.

REFERENCES

1. Rabinowitz YS. Keratoconus. *Surv Ophthalmol*. 1998;42:297–319.
2. Krachmer JH, Feder RS, Belin MW. Keratoconus and related noninflammatory corneal thinning disorders. *Surv Ophthalmol*. 1984;28:293–322.
3. Asimellis G, Kaufman EJ. Keratoconus. In: *StatPearls. Treasure Island (FL)*. StatPearls Publishing; 2024. http://www.ncbi.nlm.nih.gov/books/NBK470435/. Accessed October 29, 2024.
4. Gordon-Shaag A, Millodot M, Shneor E, et al. The genetic and environmental factors for keratoconus. *Biomed Res Int*. 2015;2015:795738.
5. Wollensak G, Spoerl E, Seiler T. Riboflavin/ultraviolet-a-induced collagen crosslinking for the treatment of keratoconus. *Am J Ophthalmol*. 2003;135:620–627.
6. Ertan A, Colin J. Intracorneal rings for keratoconus and keratectasia. *J Cataract Refract Surg*. 2007;33:1303–1314.
7. Kwitko S, Severo NS. Ferrara intracorneal ring segments for keratoconus. *J Cataract Refract Surg*. 2004;30:812–820.
8. Torquetti L, Berbel RF, Ferrara P. Long-term follow-up of intrastromal corneal ring segments in keratoconus. *J Cataract Refract Surg*. 2009;35:1768–1773.
9. Gauthier A-S, Friot M, Montard R, et al. [Femtosecond-assisted Ferrara intrastromal corneal ring implantation for treatment of keratoconus: functional outcomes at one year]. *J Fr Ophtalmol*. 2016;39:428–436.
10. Asfar KE, Bteich Y, Mrad AA, et al. Corneal allogenic intrastromal ring segments (CAIRS) versus synthetic segments: a single segment comparative analysis using propensity score matching. *J Refract Surg*. 2024;40:e863–e876.
11. Sedaghat M-R, Momeni-Moghaddam H, Piñero DP, et al. Predictors of successful outcome following intrastromal corneal ring segments implantation. *Curr Eye Res*. 2019;44:707–715.
12. Friedman JH. Greedy function approximation: a gradient boosting machine. *Ann Stat*. 2001;29:1189–1232.
13. Krizhevsky A, Sutskever I, Hinton G. ImageNet classification with deep convolutional neural networks. *Commun ACM*. 2017;60:84–90.
14. Chen T, Guestrin C. XGBoost: a scalable tree boosting system. Proceedings of the 22nd ACM SIGKDD International Conference on Knowledge Discovery and Data Mining. August 2016:785–794.
15. Sarvamangala DR, Kulkarni RV. Convolutional neural networks in medical image understanding: a survey. *Evol Intell*. 2022;15:1–22.
16. Ting DSW, Pasquale LR, Peng L, et al. Artificial intelligence and deep learning in ophthalmology. *Br J Ophthalmol*. 2019;103:167–175.
17. Lee A, Taylor P, Kalpathy-Cramer J, et al. Machine learning has arrived. *Ophthalmology*. 2017;124:1726–1728.
18. Khanthik A, Kasetsuwan N, Yaisawang S, et al. Factors predicting the visual outcome of intracorneal ring segment for keratoconus. *PLoS One*. 2024;19:e0288181.
19. Maeda N, Klyce SD, Smolek MK, et al. Automated keratoconus screening with corneal topography analysis. *Invest Ophthalmol Vis Sci*. 1994;35:2749–2757.
20. Accardo PA, Pensiero S. Neural network-based system for early keratoconus detection from corneal topography. *J Biomed Inform*. 2002;35:151–159.
21. Arbelaez MC, Versaci F, Vestri G, et al. Use of a support vector machine for keratoconus and subclinical keratoconus detection by topographic and tomographic data. *Ophthalmology*. 2012;119:2231–2238.
22. Lavric A, Valentin P. KeratoDetect: keratoconus detection algorithm using convolutional neural networks. *Comput Intell Neurosci*. 2019;2019:8162567.
23. Kamiya K, Ayatsuka Y, Kato Y, et al. Keratoconus detection using deep learning of colour-coded maps with anterior segment optical coherence tomography: a diagnostic accuracy study. *BMJ Open*. 2019;9:e031313.
24. Maile H, Li J-PO, Gore D, et al. Machine learning algorithms to detect subclinical keratoconus: systematic review. *JMIR Med Inform*. 2021;9:e27363.
25. Aatila M, Lachgar M, Hamid H, et al. Keratoconus severity classification using features selection and machine learning algorithms. *Comput Math Methods Med*. 2021;2021:9979560.
26. Afifah A, Syafira F, Afladhanti PM, et al. Artificial intelligence as diagnostic modality for keratoconus: a systematic review and meta-analysis. *J Taibah Univ Med Sci*. 2024;19:296–303.
27. Ting DSJ, Foo VH, Yang LWY, et al. Artificial intelligence for anterior segment diseases: emerging applications in ophthalmology. *Br J Ophthalmol*. 2021;105:158–168.
28. Siddiqui AA, Ladas JG, Lee JK. Artificial intelligence in cornea, refractive, and cataract surgery. *Curr Opin Ophthalmol*. 2020;31:253–260.
29. Yamauchi T, Tabuchi H, Takase K, et al. Use of a machine learning method in predicting refraction after cataract surgery. *J Clin Med*. 2021;10:1103.
30. Vega-Estrada A, Alio JL, Brenner LF, et al. Outcome analysis of intracorneal ring segments for the treatment of keratoconus based on

visual, refractive, and aberrometric impairment. *Am J Ophthalmol*. 2013; 155:575–584.e1.
31. Valdés-Mas MA, Martín-Guerrero JD, Rupérez MJ, et al. A new approach based on Machine Learning for predicting corneal curvature (K1) and astigmatism in patients with keratoconus after intracorneal ring implantation. *Comput Methods Programs Biomed*. 2014;116:39–47.
32. Lyra D, Ribeiro G, Torquetti L, et al. Computational models for optimization of the intrastromal corneal ring choice in patients with keratoconus using corneal tomography data. *J Refract Surg*. 2018;34: 547–550.
33. Ancèle E, Malecaze F, Arné J-L, et al. [Predictive factors for successful Ferrara intracorneal ring segment implantation in keratoconus]. *J Français d'Ophtalmologie*. 2011;34:513–520.
34. David C, Kallel S, Trinh L, et al. [Intracorneal ring segments in keratoconus management]. *J Fr Ophtalmol*. 2021;44:882–898.
35. Benlarbi A, Kallel S, David C, et al. Asymmetric intrastromal corneal ring segments with progressive base width and thickness for keratoconus: evaluation of efficacy and analysis of epithelial remodeling. *J Clin Med*. 2023;12:1673.
36. Lecun Y, Bottou L, Bengio Y, et al. Gradient-based learning applied to document recognition. *Proc IEEE*. 1998;86:2278–2324.
37. Prokhorenkova L, Gusev G, Vorobev A, et al CatBoost: unbiased boosting with categorical features. In: *Advances in Neural Information Processing Systems*. Vol 31. Curran Associates, Inc.; 2018. https://proceedings.neurips.cc/paper_files/paper/2018/hash/14491b756b3a51daac41c24863285549-Abstract.html. Accessed October 29, 2024.

